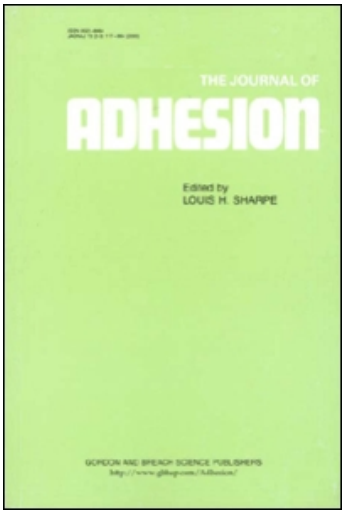

The Journal of Adhesion

Publication details, including instructions for authors and subscription information:
http://www.informaworld.com/smpp/title~content=t713453635

Elastoplastic Fracture Behavior of Structural Adhesives Under Monotonic Loading

Erol Sancaktar[a]; Hooshang Jozavi[a]; Joseph Baldwin[a]; Jing Tang[a]
[a] Department of Mechanical and Industrial Engineering, Clarkson University, Potsdam, New York, U.S.A.

To cite this Article Sancaktar, Erol , Jozavi, Hooshang , Baldwin, Joseph and Tang, Jing(1987) 'Elastoplastic Fracture Behavior of Structural Adhesives Under Monotonic Loading', The Journal of Adhesion, 23: 4, 233 — 262
To link to this Article: DOI: 10.1080/00218468708075409
URL: http://dx.doi.org/10.1080/00218468708075409

J. Adhesion, 1987, Vol. 23, pp. 233–262
Photocopying permitted by license only

Printed in the United Kingdom

Elastoplastic Fracture Behavior of Structural Adhesives Under Monotonic Loading†

EROL SANCAKTAR, HOOSHANG JOZAVI, JOSEPH BALDWIN and JING TANG

Department of Mechanical and Industrial Engineering, Clarkson University, Potsdam, New York 13676, U.S.A.

Elastic-plastic fracture behavior of a structural adhesive in the bulk and bonded forms is discussed. The model adhesive chosen, Metlbond 1113 (with scrim carrier cloth) and 1113-2 (neat resin) solid film adhesives exhibit a relatively brittle material behavior to justify the use of LEFM methods.

The solid film adhesives are first cast in the form of tensile coupons to determine the bulk fracture properties with the use of single-edge-cracked specimen geometry. K_{IC} evaluation is done using the procedure suggested by the ASTM standard. A K-calibration method based on application of boundary collocation procedure to the William's stress function is utilized to relate the measured critical loads to the K_{IC} values. The yield stresses and elastic moduli values in the bulk tensile mode are also evaluated. The availability of K_{IC}, σ_y, E and v (Poisson's ratio) values makes the calculation of crack tip plastic zone radii (r_{yc}) and fracture energy (G_{IC}) values possible on the basis of Irwin's theory. The bulk casting procedure is done under different cure (temperature, time and cool-down) conditions to determine optimum properties.

The fracture behavior of the same adhesives in the bonded form is studied with the use of Independently Loaded Mixed Mode Specimen (ILMMS) geometry. This specimen allows independent measurement of P_I and P_{II} (and consequently G_I and G_{II}) values. Since the fracture energy values are affected by the thickness of the adherend and the bondline, an experimental program is executed first by varying these geometrical parameters to determine the plane strain conditions. The relationship between the bondline thickness and the crack tip plastic zone radius values calculated earlier is also studied. Expressions developed on the basis of LEFM assumptions are utilized to calculate G_{IC} and G_{IIC} values in the bonded form. The G_{IC} values obtained in this manner are compared to the bulk G_{IC} values obtained earlier.

† Presented at the Tenth Annual Meeting of the Adhesion Society, Inc., Williamsburg, Virginia, U.S.A., February 22–27, 1987.

With the availability of P_I and P_{II} (G_I and G_{II}) values that result in failure in the bonded form, the fracture condition (i.e. the fracture failure criterion) in mixed mode (modes *I* and *II*) loading is determined for adhesively bonded joints. The use of both 1113 and 1113-2 adhesives also reveals the effects of the carrier cloth on the mechanical phenomena cited above.

KEY WORDS Elastoplastic bulk and bonded adhesive fracture; energy balance criterion; maximum principal stress criterion; independently loaded mixed mode adhesive fracture specimen; plastic deformation zone-adhesive thickness interdependence; compliance calibration.

INTRODUCTION

Adhesively bonded joint failures are usually results of catastrophic crack propagations (brittle fracture) originating from inherent flaws (voids or trapped air bubbles) and impurities.[1] These flaws are mainly formed in the bulk of the adhesive material during the curing process if ideal bonding and surface preparation of adherends prevail. Hence, a complete characterization of adhesives requires investigation of flaw-related material properties as well as bulk tensile properties as functions of cure and other service parameters. Since inherent flaws usually cause structural adhesives to fail in a brittle manner, the use of an LEFM (Linear Elastic Fracture Mechanics) method can be considered appropriate for characterizing their fracture behavior.

This paper presents data using model thermosetting adhesives Metlbond 1113 and 1113-2 which are commercially available from Narmco Materials, Inc. (Costa Mesa, California) in 0.25 mm and 0.13 mm (respectively) thick solid film rolls. Metlbond 1113 is a 100% solids, modified nitrile epoxy film with a synthetic carrier cloth. Metlbond 1113-2 is identical to 1113 matrix without the carrier cloth.

Brinson *et al.*[2] determined that the mechanical behavior of bulk Metlbond 1113 and 1113-2 adhesives is affected by the rate of straining. They showed that the constant strain rate stress–strain behavior of the adhesives approaches a perfectly elastic-plastic behavior as the magnitude of strain rate is increased. This mechanical behavior was described with the use of a modified Bingham viscoelastic-plastic model.

Since the stresses at a crack tip reach high values upon loading,

yielding occurs in a zone called the "crack tip plastic zone." If this zone is small compared to crack length, it will not greatly disturb the elastic stress field around it. Consequently, the extent of the plastic zone can be defined by the elastic stresses. Apparently, the use of an elastic-plastic material assumption in stress analysis problems greatly facilitates the solution.

The elastic-plastic material behavior assumption has been widely used for adhesive materials by a number of investigators such as Bascom[3] and Hart-Smith.[4] Bascom used a crack tip plane-strain assumption to relate the adhesive tensile yield stress, elastic modulus and the crack tip critical plastic zone radius to the fracture energy (G_{IC}). He calculated the critical plastic zone radius (r_{yc}) by using experimentally measured values of G_{IC}, σ_y and E.[3]

In order to be able to interpret the bulk data to design bonded joints, however, one needs to understand the constraint mechanism imposed on the adhesive material in the bonded form. Bascom[3] reports that the maximum fracture energy for an adhesive in the bonded form was obtained when the bond thickness was approximately equal to the critical plastic zone diameter ($2r_{yc}$). His investigations also revealed that this maximum G_{IC} value was equal to that obtained with the bulk form of the adhesive.

In adhesively bonded joints crack propagation is constrained within the adhesive layer regardless of the loading orientation. Because of this condition one needs to consider mixed mode fracture. The majority of practical adhesive applications involve only G_I and G_{II} due to the peel and in-plane-shear stresses that arise in the use of lap joint geometries. In such geometries, adhesive cracks are exposed to both tension and shear resulting in mixed mode cracking.

The Independently Loaded Mixed Mode Specimen (ILMMS) geometry is used during the current investigation for mixed mode testing of adhesives in the bonded form. This geometry was originally proposed by Ripling *et al.*[5] It allows simultaneous but physically separate application of cleavage and shear loads. Monotonic loading of the specimens with different P_I to P_{II} ratios enables us to determine the failure criterion for fracture of adhesively bonded specimens.

In order to determine the fracture toughness (K_{IC}) of bulk adhesives, the single-edge-cracked specimen geometry shown in

Figure 1 was chosen. The pertinent dimensions of plate specimens for K_{IC} testing are the crack length, thickness and the ligament (uncracked) length. According to ASTM standards,[6] for a K_{IC} test to be valid, these dimensions should exceed a certain multiple of the quantity $(K_{IC}/\sigma_y)^2$. This quantity has been shown[6] to be directly proportional to the radius of the crack tip critical plastic zone. Based on the elastic-plastic material assumption, the LEFM solutions are valid beyond the plastically deformed zone around the crack tip, if the size of this zone is small.

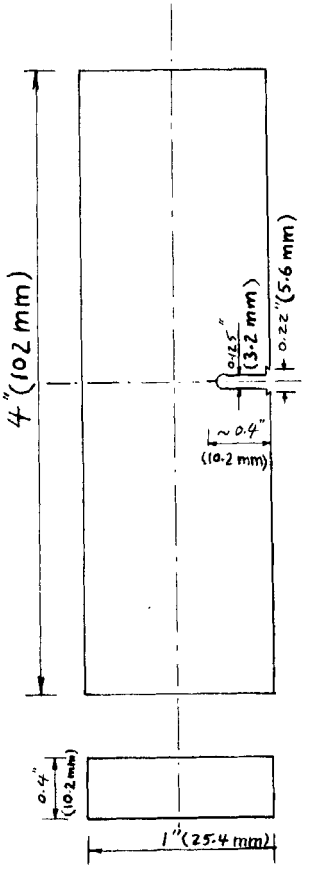

FIGURE 1 Single-edge-cracked specimen geometry used for fracture toughness (K_{IC}) measurements.

Based on the above considerations, this paper presents elastoplastic fracture behavior of a model solid film epoxy adhesive (Metlbond) with (1113) and without (1113-2) carrier cloth using bulk and bonded specimens. The bulk specimens are tested under monotonic loading using single-edge-crack specimen geometry. The Independently Loaded Mixed Mode specimen (ILMMS) geometry is used for mixed mode testing in the bonded form. In both cases, a high rate of monotonic loading is used to achieve an approximate elastic-plastic material behavior since the mechanical behaviors of the model adhesives were shown to approach elastic-plastic behavior at high strain rates.[2]

The solid film adhesives are first cast in the form of tensile coupons to determine the bulk fracture properties under monotonic loading with the use of single-edge-crack specimen geometry. K_{Ic} evaluation is done using the procedure suggested by the ASTM standard. A K-calibration method based on application of boundary collocation procedure to the William's stress function is utilized to relate the measured critical loads to the K_{IC} values. The yield stresses and elastic moduli values for the model adhesives in the bulk tensile mode have already been evaluated by Sancaktar *et al.* and reported in the literature.[7] The availability of K_{IC}, σ_y, E and v (Poisson's ratio) values makes the calculation of crack tip critical plastic zone radii (r_{yc}) and fracture energy (G_{IC}) values possible on the basis of Irwin's theory.[8] The effects of cure time, temperature and cool-down conditions on r_{yc} and G_{IC} are also illustrated and the (optimum) cure conditions resulting in the maximum r_{yc} and G_{IC} values are evaluated. These cure conditions are used in curing of bonded samples.

The fracture behavior of the model adhesives in the bonded form is studied with the use of Independently Loaded Mixed Mode Specimen (ILMMS) geometry. Since the fracture energy values are affected by the thickness of the adherend and the bondline, an experimental program is executed first by varying these geometrical parameters to determine the plane strain conditions. The relationship between the bondline thickness and the crack tip plastic zone radius values calculated earlier with the use of bulk data is also studied. Expressions developed on the basis of LEFM assumptions are utilized to calculate G_{IC} and G_{IIC} values in the bonded form. The G_{IC} values obtained in this manner are compared to the bulk G_{IC} values obtained earlier.

With the availability of P_I and P_{II} (G_I and G_{II}) values that result in failure in the bonded form, the fracture condition (*i.e.*, the fracture failure criterion) in mixed mode (modes *I* and *II*) loading is determined for adhesively bonded joints. For this purpose, energy balance and maximum principal stress criteria are used.

The use of model adhesives Metlbond 1113 (with carrier cloth) and 1113-2 (neat resin) also reveals the effects of the carrier cloth on the mechanical phenomena cited above.

ANALYTICAL CONSIDERATIONS

Irwin[8] showed that for an isotropic material in the bulk form and crack tip plane strain conditions, the stress intensity factor can be expressed as

$$K_I = (G_I E/1 - \upsilon^2)^{1/2} \tag{1}$$

where υ is the Poisson's ratio.

For ductile materials the crack propagation process involves mainly plastic energy due to crack tip plastic deformation. Furthermore, the mathematical formulation of the stress field based on perfectly elastic material behavior suffers from singularity at the crack tip. In order to resolve this problem, Irwin assumed elastic-plastic material behavior and stated that the failure stress at the crack tip is equal to the uniaxial yield stress acting over a region called the plastic zone. Beyond this zone the elastic stress distribution remains undisturbed. Irwin[8] calculated the size (diameter) of the plastic deformation zone by considering an infinite plate containing a single crack under the action of tensile in-plane loading perpendicular to the crack. The diameter of the plastic (deformation) zone was thus shown to be

$$r_p = K_{IC}^2/\pi\sigma_y^2. \tag{2}$$

Based on Eqs. (2) and (1), the "corrected" critical strain energy release rate could then be written as

$$G_{IC} = \pi\sigma_y^2 r_p(1 - \upsilon^2)/E. \tag{3}$$

Irwin showed that the plane-strain elastic constraint will increase the tensile yield stress for plastic yielding and thus affect the size of

the plastic zone. Such an increase in the yield strength was estimated to be by a factor of approximately the square root of 3.[8,9] The critical radius of the crack tip deformation zone can, therefore, be written as

$$2r_{yc} = (1/\pi)\{K_{IC}/(3)^{1/2}\sigma_y\}^2 \tag{4}$$

for plane-strain conditions. Substitution into Eq. (1) results in

$$G_{IC} = 6\pi\sigma_y^2 r_{yc}(1 - \upsilon^2)/E. \tag{5}$$

For an elastic cracked structure subjected to some mode I load (P_I), the rate of strain energy release (G_I) has been related to the material and geometrical properties and applied load[9] with the equation

$$G_I = (P_I^2/2b)(\partial c/\partial a) \tag{6}$$

where b = material thickness in the vicinity of crack ($b = 10.2$ mm in Figure 1), $\partial c/\partial a$ = change in compliance (c) with crack length (a), ($a = 10.2$ mm in Figure 1).

The load level at which spontaneous crack growth occurs is called the critical load (P_c) and the corresponding energy release rate is called the fracture energy (G_c).

In order to utilize Eq. (6) one needs to determine the variation of compliance (ratio of displacement to the applied load) for different crack lengths of a given specimen geometry.

Determination of fracture energy in bonded and bulk samples

A. Bonded samples

There are three basic specimen geometries for mixed mode testing of adhesives in the bonded form. They are cracked lap-shear,[10] scarf joint[11] and the Independently Loaded Mixed Mode Specimen (ILMMS) geometries. Among these, the only specimen geometry which allows independent measurement of P_I and P_{II} (and consequently G_I and G_{II}) is the ILMMS. The other two require finite element analysis to calculate G_I and G_{II} values from a load applied in only one direction. In order to avoid any inaccuracies which may be involved in the calculation of G_I and G_{II} values with the use of a

finite element program and due to its practicality in load measurement, the ILMMS geometry is used during the current investigation. In order to test different P_I to P_{II} ratios, a hydraulic actuator force is applied statically in mode *II* and the specimen is loaded monotonically in mode *I* until failure. Subsequently, the static force is applied in mode *I* while the specimen is loaded monotonically in mode *II* until failure.

Examination of the literature and our experience show that the strain energy values are affected by the thickness of the adherend and the bondline. For this reason it is necessary first to determine, experimentally, the adhesive and adherend thickness values that result in plane strain conditions. The following methods are used for this purpose:

As mentioned earlier, Bascom[3] reports that the maximum fracture energy for an adhesive in the bonded form is obtained when the bond thickness is approximately equal to the critical plastic zone diameter ($2r_{yc}$). His investigations also reveal that this maximum G_{IC} value is equal to that obtained with the bulk form of the adhesive.

Limited information is available in the literature regarding the effects of adherend thickness (b) (or crack front length) on G_{IC}. Kinloch *et al.* report that the stress condition at the crack tip of an adhesive bond varies from one of plane stress for short crack fronts (thin bonds) and at the edges of thicker bonds, to one of plane strain near the center of thick bonds. The increased constraint present in plane strain conditions results in a smaller zone of plastic deformation.[12] This indicates that as the adherend thickness increases, thereby increasing constraint on material deformation, the fracture energy will decrease.

The advantage in using the ILMM specimens is the option of not having to calculate G_I or G_{II} values in order to determine the fracture criterion. The availability of separate P_I and P_{II} values is sufficient to obtain such a criterion. However, calculation of G_I and G_{II} values is helpful in accounting for geometrical effects (when different geometries are used) and for comparison purposes.

Our experiments showed that P_{IIC} is a (linear) function of the bond length (L), ($L = 12.7$ cm in Figures 2 and 3) and therefore necessary terms must be included in any G_{IIC} relation to render this material constant (G_{IIC}) independent of geometrical effects. For this

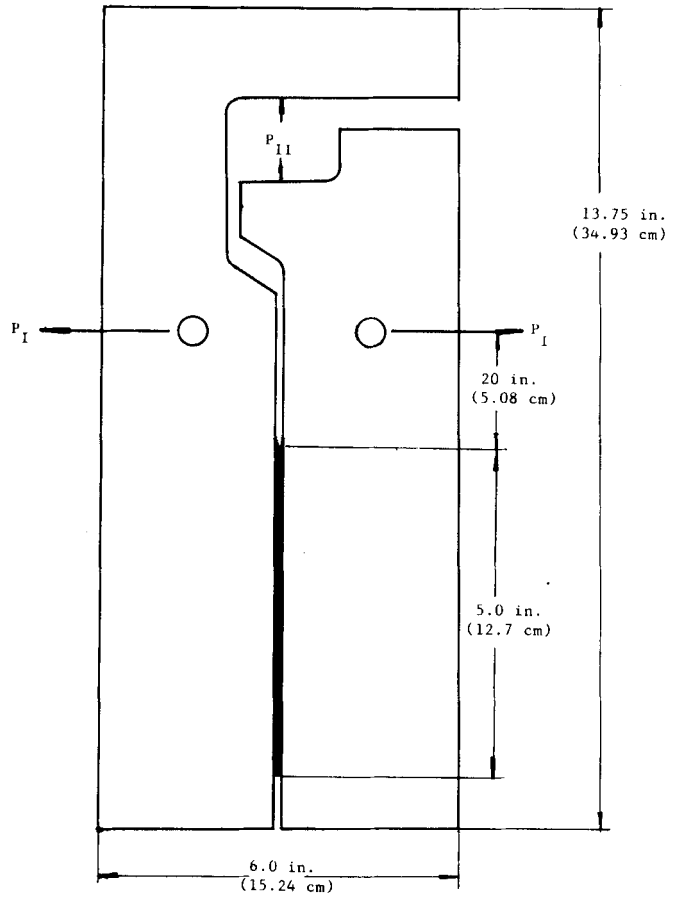

FIGURE 2 ILMM specimen geometry *A* for monotonic opening, static in-plane shear loading.

purpose, the following simplified approach is used: If we assume that in an ILMM specimen the axial load varies linearly along the overlap direction[13] then the total elastic energy (W_T) stored in the adhesive and the adherends can be written as

$$W_T = \int_0^L \int_0^h \int_0^b (P_{II}^2/E_{st}h^2b^2)(1 - y/L)^2 \, dx \, dy \, dz + (nbL)(\tau_{avg}^2/2G_A) \tag{7}$$

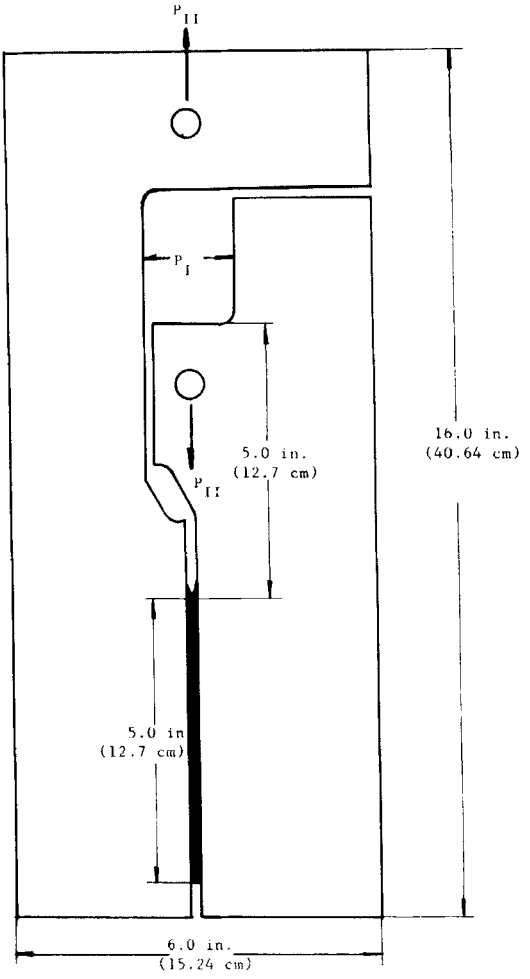

FIGURE 3 ILMM specimen geometry *B* for monotonic in-plane shear static opening loading.

where, h = adherend beam height ($2h = 15.24$ cm in Figures 2 and 3), E_{st} = Young's modulus for the steel adherends, n = adhesive thickness, G_A = elastic shear modulus for the adhesive, and $\tau_{avg} = P_{II}/Lb$ = average shear stress in the adhesive layer. Solution of Eq. (7) with the assumption

$$G_{II} = W_T/2Lb \tag{8}$$

yields

$$G_{II} = (P_{II}^2/2b^2)(1/3hE + n/2L^2G_A). \quad (9)$$

Note that Eq. (9) accommodates the linear increase of P_{II} with L.

A widely accepted relation for G_I in (bonded) double cantilever beam specimens is

$$G_{IC} = 4P_{IC}^2(3(a + a_0)^2 + h^2)/b^2h^3E. \quad (10)$$

Experimentation shows that in addition to bending and shear deflections, there exists additional deflection due to rotation at the assumed "built in" end of the beam. It is assumed that this rotation can be treated as an increase in crack length and hence it is accounted for with the use of the empirical rotation factor a_0 in Eq. (10). The value of a_0, however, must be determined experimentally when the geometrical parameters are varied. This is accomplished by means of experimental compliance calibration.

B. Bulk samples

For the single-edge-crack geometry used for bulk samples, Gross *et al.*[14] applied a boundary collocation procedure to the William's stress function to determine the elastic stress distribution at the tip of an edge crack in a finite-width specimen subjected to uniform tensile loading. The K-calibration for the single-edge-crack geometry is given by:

$$K_{IC}bw/P_Ca^{1/2} = 1.99 - 0.41(a/w) + 18.7(a/w)^2 - 38.48(a/w)^3 + 53.85(a/w)^4 \quad (11)$$

where w is the specimen width. Examination of the literature[6] reveals that in single-edge-crack samples a plane strain condition is ensured when the minimum values for specimen thickness (b) and crack length (a) are given by:

$$a, b \geq 2.5(K_{IC}/\sigma_y)^2. \quad (12)$$

Determination of failure criterion

With the application of the energy balance criterion we get:

$$K_I^2 + K_{II}^2 = \text{constant} \quad (13)$$

where the locus of failure is a quarter circle. However, previous

experimentation by other researchers[15] showed that an elliptical condition is more realistic, *i.e.*

$$(P_I/P_{IC})^2 + (P_{II}/P_{IIC})^2 = 1. \tag{14}$$

A second criterion that must be considered involves the possibility of failure in mode *I* under the action of the maximum principal stress since a biaxial state of stress is applied globally. It should be noted that the mode *I* in such cases will be at angle to the applied P_I load, with this angle being determined by the applied P_I to P_{II} ratio. Obviously, such an inclined crack will have to connect with similar ones or simply continue propagating in the P_{II} direction (possibly close to or at the interface) to result in catastrophic failure. The likelihood of this type of failure is high, especially for brittle adhesives.

We propose the following simplified approach to describe this type of failure: If one takes a biaxial stress element well ahead of the crack tip where the stresses are defined and uniform, then the elementary theory defines the maximum principal stress as:

$$(\sigma/2) + [(\sigma^2/4) + \tau^2]^{1/2} = \text{constant} \tag{15}$$

Assuming that loads and stresses are linearly related, substitution into Eq. (15) yields:

$$CAP_I + B^2P_{II}^2 = C^2. \tag{16}$$

Note that Eq. (16) describes a parabolic failure condition while Eq. (14) described an elliptical one. Obviously Eq. (16) should contain at least an additional P_I^2 term resulting from the contribution of shear loading to the opening direction. However, this contribution is neglected, as it is assumed to be small.

It should also be noted that Eq. (16) can be rewritten in terms of the stress intensity factors as:

$$(K_I/K_{IC}) + (K_{II}/K_{IIC})^2 = 1 \tag{17}$$

EXPERIMENTAL PROCEDURES

Bulk samples[16]

Metlbond 1113 and 1113-2 adhesive rolls were stored in a freezer at −1°C and 0% *RH*. First, the adhesive roll was taken out of the

freezer and allowed to thaw in the ambient temperature until it was flexible enough to work with. It was determined that for Metlbond 1113 (with carrier cloth) 45 layers and for Meltbond 1113-2 (without carrier cloth) 78 layers were needed to make thickness of 10.16 mm of cured material. Each layer was cut to 38 mm × 330 mm size. Two aluminum plates with 5 mm × 38 mm × 330 mm grooves were sprayed with Teflon® and were used to cast the multilayered adhesive. For this purpose, the adhesive layers were carefully laid on one grooved plate and smoothened. The second plate was then placed on top of the first one and the two plates were tightly and uniformly clamped together. The assembly was subsequently placed in the oven for curing.

At the end of the cure cycle, the assembly was cooled either quickly or slowly to simulate the fast and slow cool-down conditions.

For each cure condition three specimens were manufactured. In order to facilitate the machining of the specimens, the cured adhesive plate was taped to a metal specimen template using two-sided tape. A vertical contour saw was used to remove most of the excess adhesive along the template border. The final contour shaping was done by using a carbide-bit router as the template slid along a guide pin to ensure a uniform specimen shape. Finally, the surfaces of the specimen were smoothened with a fine grade sanding block. The starter crack was produced subsequently by tapping a sharp knife at the base of the machined notch. The knife-edge at the mouth of the machined notch (Figure 1) was made to facilitate mounting of a Crack Opening Displacement (C.O.D.) gage which was used in determining the K_{IC} values. The final specimen dimensions are shown in Figure 1.

Several measurements had to be made before testing a specimen. The width and thickness were accurately measured using a micrometer. The total crack length (including the depth of machined notch and starter crack) was measured using a light reflective microscope at a magnification of 10×. This was done on both sides of the specimen and an average crack length value was calculated.

Bonded samples

The original dimensions and geometry proposed by Ripling and Mostovoy were altered substantially, on the basis of our experimen-

tal stress analysis through the use of reflection and transmission photoelasticity in order to minimize any interference between the two modes (*i.e.*, cleavage loads resulting from shear loads, etc.) and to reduce the effects of stress discontinuities. This new geometry allows the use of a small hydraulic actuator inside the specimen. The geometries developed are shown in Figures 2 and 3. Since the width of the actuator used is larger than its height, it was necessary to develop two different specimen geometries with geometry *A* (Figure 2) being used for static loading in mode *II* and geometry *B* used for static loading in mode *I*. Examination of Figures 2 and 3 reveals the presence of frictional resistance affecting the loads applied orthogonal to the static loads. These frictional loads were measured experimentally and subtracted from the applied (monotonic) loads. Even though the frictional resistance existed only in the sliding mode during all our experiments, the validity of the subtraction procedure based on static equilibrium was checked with the use of rolling friction. For this purpose steel pins were placed in between the actuator face and the specimen. In both sliding and rolling friction cases the same G_I and G_{II} ratios were obtained corresponding to the same crack opening displacements and also at failure.

Bonded specimen preparation

There are three major steps to bonded specimen preparation. They are:

A. Pre-etch preparation

Original specimens are cut from cold rolled 1095 steel flat stock. Specimens are reused by grinding off the old adhesive with a belt sander. With the use of 1095 grade steel, any permanent deformation of the adherends is avoided. The difference in surface roughness provided by belt sanding and milling is found to have no measurable effect on bond strength. Specimen dimensions and bond line alignment should be checked prior to the etching procedure since, after etching, handling must be kept to a minimum. Bonding surfaces should align squarely.

It is very important for the specimens to be thoroughly degreased

prior to etching. Any cutting oils left on the specimen when it is inserted into the acid bath will linger as a film on the surface of the bath and redeposit itself on the specimen as it is removed from the bath. Acetone and trichloroethane are both effective degreasing agents. A simple check to determine whether a specimen has any residual grease or oils on it is to dip it into water. If the entire surface wets, that is if a thin film of water remains on the specimen when it is taken out of the water, then it has been thoroughly degreased. However, if dry areas break out on the specimen, this indicates an oil residue and the specimen should be degreased.

B. Acid bath etching

The standard etching procedure for steel, provided by Narmco Corporation, is employed. The acid bath consists of:

150 ml sulfuric acid	7.5% by volume
300 ml nitric acid (70)	15% by volume
25–50 ml powdered sodium dichromate	5% by volume
1500 ml tap water	72.5% by volume.

The above solution is combined in a Pyrex baking dish large enough to hold both halves of a specimen. The specimens are etched one at a time at room temperature for about 2 minutes. This work must be done under a hood because of the noxious fumes given off by the reaction. Acid resistant gloves are used to handle the specimens while they are in the acid. At the end of the etching period, the specimen is removed from the bath and placed in a bucket of tap water until it can be rinsed under running water. The water rinse is needed to remove the significant oxidation layer that is formed on the specimen while in the acid bath. In fact, in order to get the specimen really clean, a Scotchbrite® pad is used and the specimen is scrubbed rigorously under running water. Care is taken to insure that no soap residue is introduced during this scrubbing.

Finally, the specimens are wiped dry with clean paper towels and baked in a 49°C oven for 15 minutes to drive off any surface moisture. If the specimens are allowed to air dry as recommended by Narmco, a thin oxidation film results. At this point, the specimens are placed in a protective enclosure (a steel tool box) for transportation and storage until they can be bonded. Bonding

should proceed as soon after etching as possible, certainly within 24 hours.

C. Bonding

It was observed that the bonding procedure was the most sensitive, and therefore the most difficult, to accomplish successfully when compared with the other steps in specimen preparation. Temperature, humidity, cleanliness, and clamping pressure are all important parameters.

To begin with, the working area must be uncluttered and dust free. It is recommended that surgical gloves be worn to eliminate the transfer of any oils or moisture from the skin to the bonding surface.

The ambient temperature of the bonding area should be high enough to soften the adhesive, making it somewhat tacky. A temperature between 21°C and 29°C allows the adhesive to be applied with a minimum of difficulty and without air inclusions. The specimens should not be cooler than the bonding environment. If cooler specimens are introduced to the bonding environment surface condensation of moisture could result.

Although 6 layers of Metlbond 1113-2 adhesive should have been enough to provide 0.64 mm bondline thickness used, it was soon discovered that double that amount of adhesive was needed to provide enough pressure to ensure a good bond. The majority of Metlbond 1113-2 tests were done with 13 layers of adhesive. For bonding with the Metlbond 1113 adhesive, 7 layers were sufficient due to the presence of the carrier cloth. The reason for the use of 0.64 mm bondline thickness will be explained later.

After the adhesive had been applied on one side of the specimen the two halves are joined and placed in a bonding jig. Teflon coated steel spacing shims are placed at either end of the bond and clamping pressure is applied.

All four specimens are then placed in an oven set at 149°C for 30 minutes. The specimens are allowed to cool slowly (usually overnight) by turning off the oven an leaving the door closed.

Once cool, excess adhesive is filed off the sides of the specimens and bondline measurements are taken. The specimens are then ready for testing.

Both bulk and bonded specimens were tested under monotonic tension with a constant crosshead rate of 50.8 mm/min. Such a fast head rate was used to minimize the viscoelastic effects.

RESULTS AND DISCUSSIONS

Bulk samples

As mentioned earlier, information on the size of the crack tip critical plastic zone radius makes it possible to relate the bulk properties to fracture properties in the form of fracture toughness and fracture energy. Such a relation is possible on the basis of a "small scale" yielding assumption[11] and Eqs. (5) and (1). Figures 4 and 5 show the effects of cure conditions on the (calculated) critical plastic zone radius of Metlbond 1113 and 1113-2, respectively. Examination of these figures reveals that r_{yc} values corresponding to optimum K_{IC}'s for the fast or slow cool-down conditions are relatively constant. Therefore, it seems possible that one can use some average r_{yc} values (based on optimum K_{IC}'s) to represent the

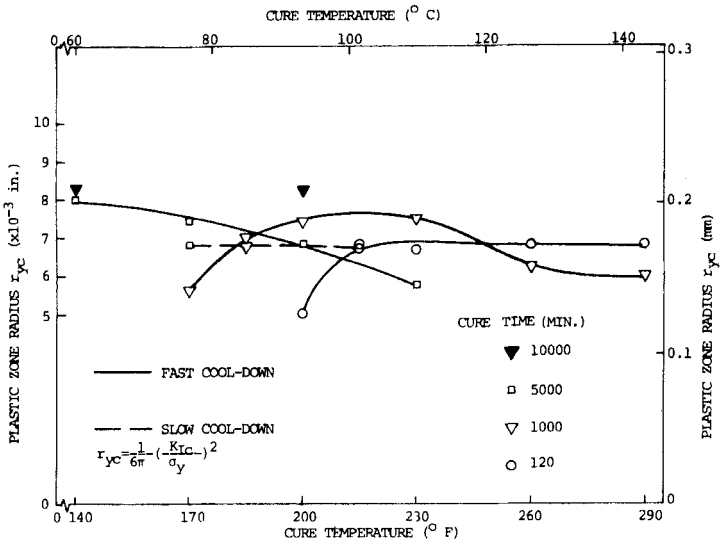

FIGURE 4 Effect of cure conditions on the plastic zone radius based on bulk tensile and fracture toughness data of Metlbond 1113.

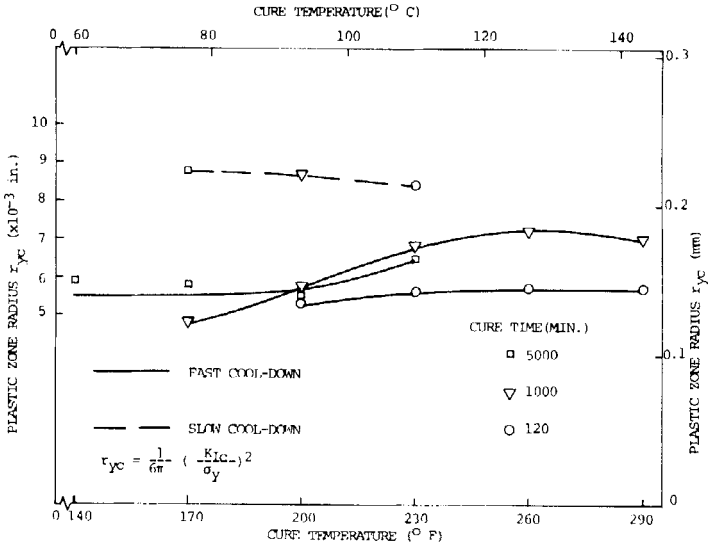

FIGURE 5 Effect of cure conditions on the plastic zone radius based on bulk tensile and fracture toughness data of Metlbond 1113-2.

typical critical plastic zone radii sizes for either material subjected to the fast or slow cool-down conditions. Using this concept, it can be seen in Figure 5 that the average critical plastic zone radius for Metlbond 1113-2 with the slow cool-down condition is higher than that for the fast cool-down condition. As expected, this implies that the slow cool-down condition results in a tougher adhesive matrix material, as the availability of a larger plastic zone size at the crack tip enables relieving of higher stress levels at that location thus resulting in higher crack growth resistance. It is not possible to offer a similar argument for the adhesive with the carrier cloth as the values obtained with slow and fast cool-down conditions are about the same (Figure 4). This result, however, is also expected since it is already known that the effect of cool-down conditions on Metlbond 1113 fracture toughness is minimal as attributed to the presence of the carrier cloth.[16]

The availability of these average r_{yc} values along with previously measured σ_y and E data made the calculations of G_{IC} values possible based on Eq. (5). These calculated values could also be

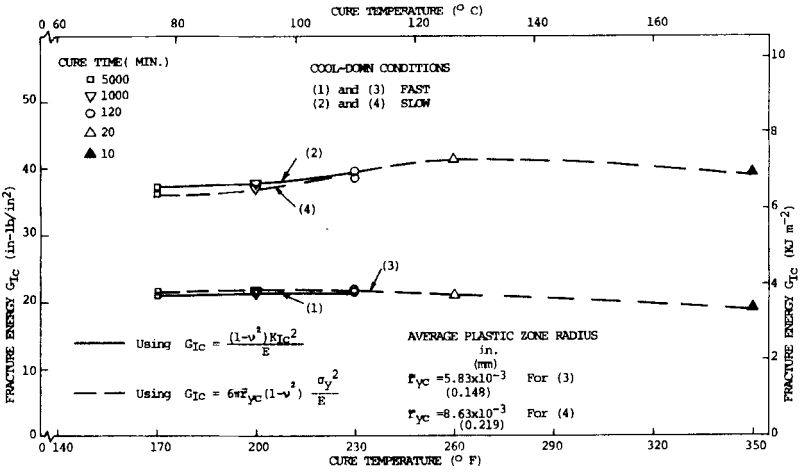

FIGURE 6 Metlbond 1113-2, slow and fast cool-down fracture energy-cure optimization curves calculated based on bulk tensile and fracture toughness data.

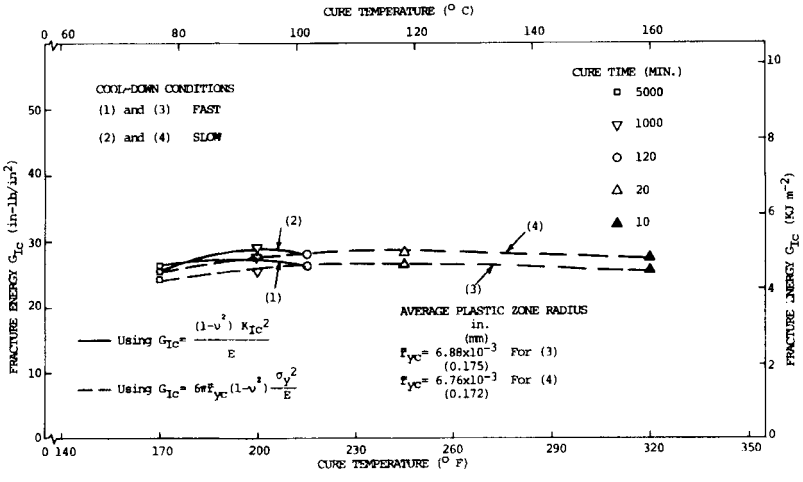

FIGURE 7 Metlbond 1113, slow and fast cool-down, fracture energy-cure optimization curves based on bulk tensile and fracture toughness data.

compared with the G_{IC} values which were obtained on the basis of measured K_{IC} values and Eq. (1) to verify the validity of using an average r_{yc} value in Eq. (5). In calculating fracture energies the value of Poisson's ratio (v) was assumed to be the constant value of 0.374 for both materials.[2] Figures 6 and 7 show the effects of cure conditions on the fracture energy of Metlbond 1113-2 and 1113, respectively. Comparison of Figures 6 and 7 confirms that: i) With the fast cool-down condition Metlbond 1113 yields higher G_{IC} values than Metlbond 1113-2; ii) With the slow cool-down condition the optimum G_{IC} values are significantly higher using Metlbond 1113-2 as compared with Metlbond 1113; iii) Cure temperature and time do not seem to have a significant effect on fracture energy for either material.

Bonded samples

Experimental results indicate that for the adhesive without the carrier cloth the G_{IC} values are maximum when the adherend thickness (b) is equal to 6.35 mm. A plane strain condition is attained when $b = 1.27$ cm (Figure 8). For the adhesive with the carrier cloth (1113) the G_{IC} value is maximum when $b = 3.18$ mm

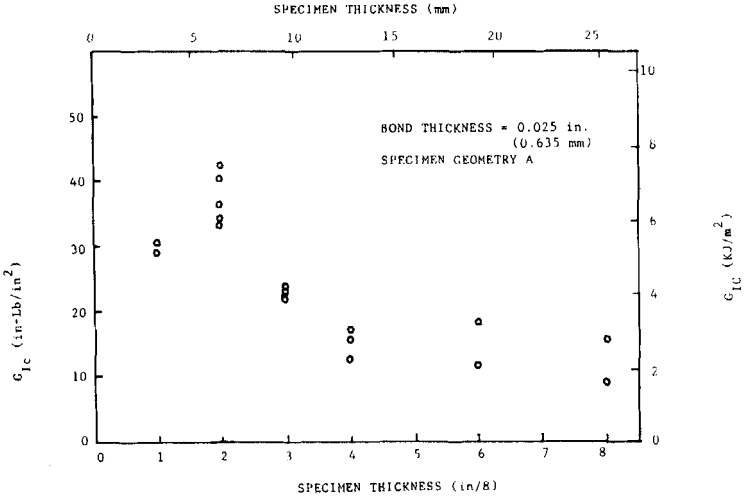

FIGURE 8 Variation of G_{IC} with specimen thickness for 1113-2 adhesive.

and the plane strain condition is attained when $b = 9.53$ mm (Figure 9). For both adhesives $b = 1.27$ cm is used for the plane strain condition. It should be noted that the maximum G_{IC} values obtained with 1113-2 and 1113 adhesives are close to the G_{IC} values previously measured by us[16] using bulk edge-crack compact tension specimens and the values measured by O'Conner[17] using bonded Tapered Double Cantilever Beam (TDCB) specimens.

As mentioned earlier, Bascom[3] reports that the G_{IC} values in the bonded form are maximum and equal to bulk G_{IC} values when the bond thicknesses (n) are equal to $2r_{yc}$. Our experimental results showed further confirmation of this assertion. For 1113-2 samples with $b = 6.35$ mm and $b = 1.27$ cm adherend thicknesses, G_{IC} is maximized and remains constant when the plane strain condition is attained slightly above the $n = 0.508$ mm value (Figures 10, 11). The adhesive thickness corresponding to the onset of the plane strain condition is close to the $2r_{yc}$ value calculated by us based on our previous bulk fracture tests[16] (Figure 5). For the adhesive with the carrier cloth the plane strain condition is achieved slightly above $n = 0.254$ mm. This value is very close to our previously calculated $2r_{yc}$ value for the 1113 adhesive[16] (Figure 4). These results also reveal the stabilizing effect of the carrier cloth on G_{IC} values.

In order to be able to use Eq. (10) in determining G_{IC} values, it is

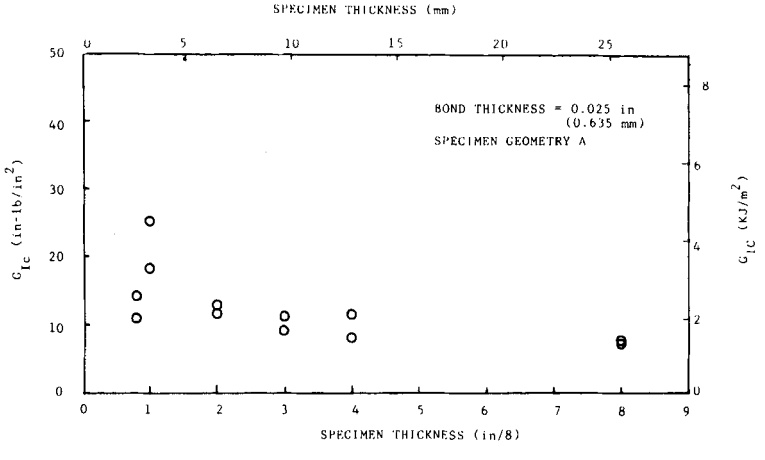

FIGURE 9 Variation of G_{IC} with specimen thickness for 1113 adhesive.

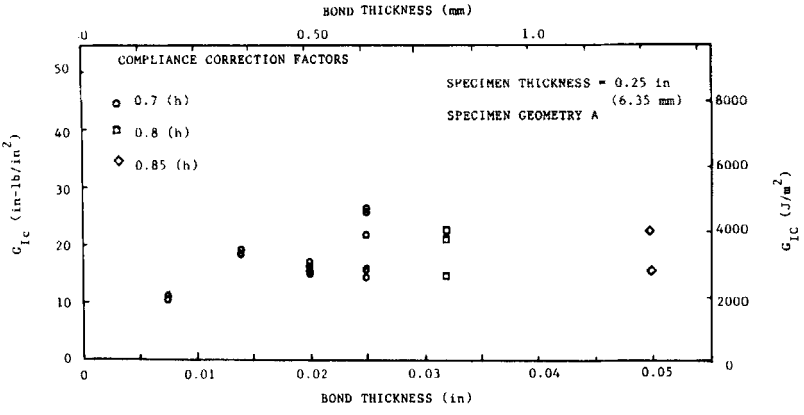

FIGURE 10 Variation of G_{IC} with bond thickness for 1113-2 adhesive.

necessary to evaluate first the rotation factor a_0 experimentally. This is done by means of compliance calibration: The specimen compliance (c) is defined as

$$c = \delta / P \tag{18}$$

where δ = crack opening displacement and P = applied opening load. Apparently, if δ *vs.* P values are determined for different

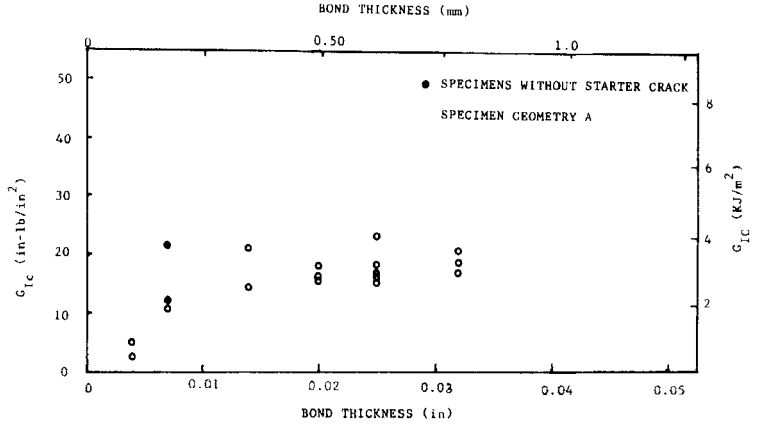

FIGURE 11 Variation of G_{IC} with adhesive thickness for 0.5 in (12.7 mm) thick specimens bonded with 1113-2 adhesive.

crack lengths then the compliance equation

$$C = (2/3EI)[(a + a_0)^3 + h^2 a] \tag{19}$$

can be fitted to these data by using the appropriate a_0 value. Figure 12 shows such compliance calibration curves for different adherend thicknesses of specimen geometry A bonded with 0.635 mm thick Metlbond 1113-2 adhesive. Obviously, for geometry A with $6.35\text{ mm} \leq b \leq 12.7\text{ mm}$, the correction factor a_0 is $(0.7)h$ where h is the beam height. Other rotation factor (a_0) values were obtained by means of compliance calibration for different adherend thicknesses, adhesive thicknesses, specimen geometries (A or B) and adhesive types (with or without carrier cloth) as shown below:

1) For the adhesive without the carrier cloth (1113-2):
   i) For geometery A with $6.35\text{ mm} \leq b \leq 12.7\text{ mm}$ (adherend thickness) and $0.178\text{ mm} \leq n \leq 0.635\text{ mm}$ (adhesive thickness): $a_0 = (0.7)h$.
   ii) Same as in 1-i except $n = 1.27$ mm: $a_0 = (0.85)h$.
   iii) For geometry b with $6.35\text{ mm} \leq b \leq 12.7\text{ mm}$ with $n = 0.635$ mm: $a_0 = (0.6)h$.

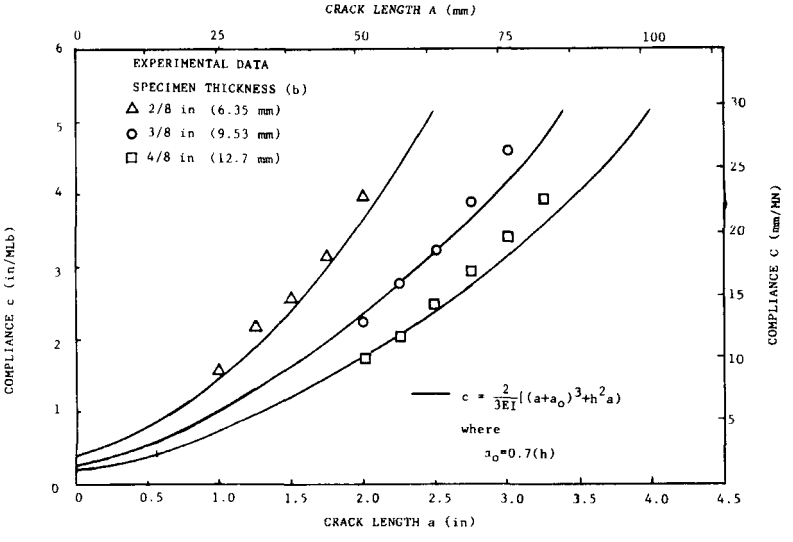

FIGURE 12 Compliance calibration for different thicknesses of geometry A bonded with 0.025 in (0.635 mm) thick 1113-2 adhesive.

2) For the adhesive with the carrier cloth (1113):
   i) For geometry *A* with $b = 6.35$ mm and $n = 0.63$ mm: $a_0 = (0.6)h$.
   ii) Same as in 2-i except $b = 12.7$ mm: $a_0 = (0.8)h$.
   iii) For geometry *B* with $b = 12.7$ mm and $n = 0.635$ mm: $a_0 = (0.8)h$.

It should be noted that some of the a_0 values reported above may be in error by as much as 25% due to experimental difficulties and functional dependence of a_0 on crack length.

Another geometrical consideration in fracture energy calculations involves the effect of bondline length on G_{II} values. Our experiments with double cantilever beams revealed that the mode *II* breaking force (P_{IIC}) increases with increasing bond length. This behavior was observed with two different beam thicknesses ($b =$ 6.35 mm and 12.7 mm) and appeared to be a linear function between the P_{IIC} and the bond length (L) (Figure 13).

Failure criteria data and curves showing P_I *vs.* P_{II} for 1113-2 and 1113 adhesives are depicted in Figures 14 through 16. Results obtained using geometry *A* (monotonic in opening, static in shear) and *B* (monotonic in shear and static in opening) are combined in these figures. Since the two geometries have different crack lengths (5.08 cm for geometry *A* and 15.24 cm for geometry *B*), opening

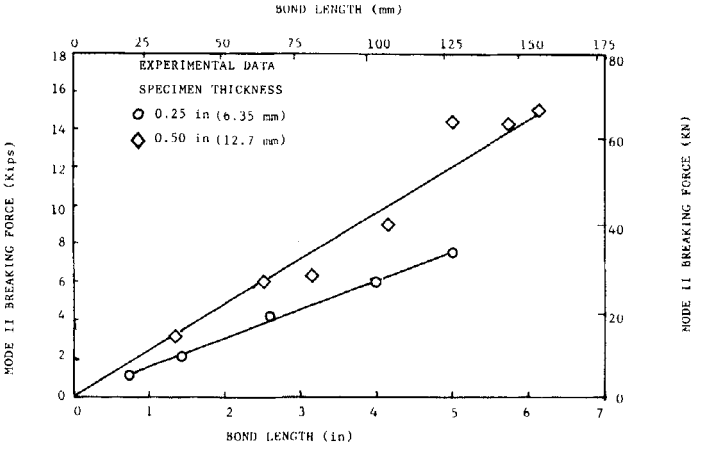

FIGURE 13 Variation of mode *II* breaking force with bond length.

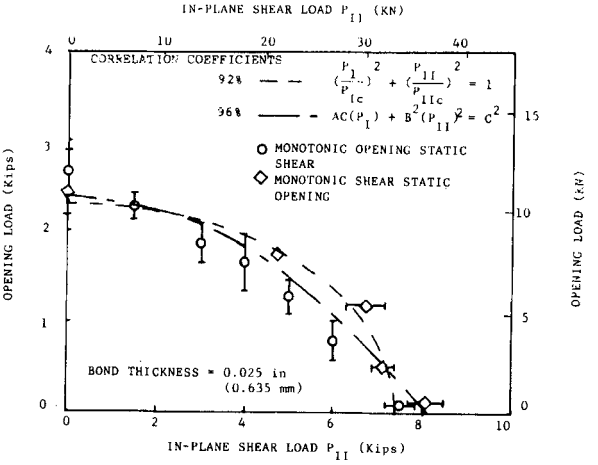

FIGURE 14 Opening load *vs.* in-plane shear load for 0.25 in (6.35 mm) thick 1113-2 ILMM specimens and comparison with theory.

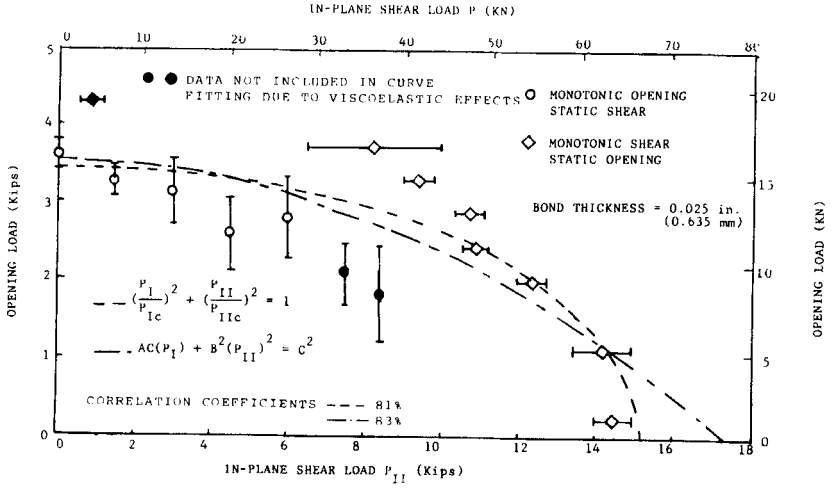

FIGURE 15 Opening load *vs.* in-plane shear load for 0.5 in (12.7 mm) thick 1113-2 ILMM specimens and comparison with theory.

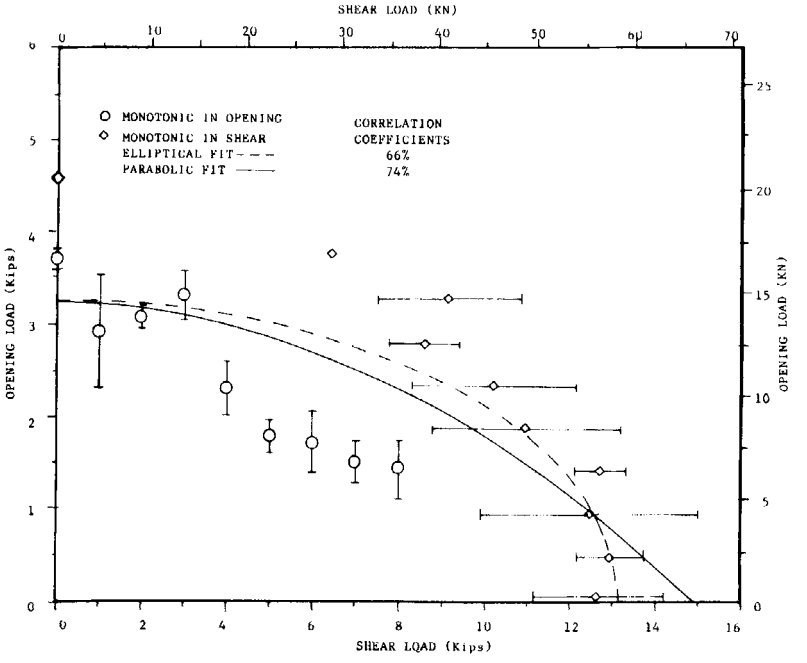

FIGURE 16 Opening load *vs.* in-plane shear load at fracture for 0.5 in (12.7 mm) thick 1113 ILMM specimens and comparison with theory. The adhesive bond thickness is 0.025 in (0.635 mm).

mode loads for geometry *B* were normalized with respect to those obtained with geometry *A*. This was done with the application of the G_I relation (Eq. (10)). The data shown in Figures 14 and 15 were obtained with the adhesive without the carrier cloth using specimens with 6.35 mm and 12.7 mm thick adherends respectively. The data for the adhesive with the carrier cloth is shown in Figure 16 for the adherend thickness of 12.7 mm. Included in these figures are also correlation coefficients to indicate the goodness of fit for elliptical (Eq. (14)) and parabolic (Eq. (16)) functions based on energy balance and principal stress criteria respectively.

Comparison of Figures 15 and 16 reveal that larger P_I and/or P_{II} loads (and consequently the corresponding fracture energy values) are required for the failure of *ILMM* specimens bonded with the adhesive without the carrier cloth (Metlbond 1113-2) in comparison

to the samples bonded using the adhesive with the carrier cloth (Metlbond 1113). This result is in agreement with the results of our bulk fracture experiments where higher G_{IC} values were obtained for Metlbond 1113-2 in comparison to Metlbond 1113. Note that this comparison between the bulk and bonded samples is made only for the samples that have matching cure conditions with the slow cool-down condition being the most important.

The experimental results also reveal more randomness and hence more data scatter in the bonded fracture behavior of the adhesive with the carrier cloth in comparison to the fracture behavior of the neat resin.

Examination of Figures 14 through 16 also reveal two important points common to all of them:

1) The presence of viscoelastic effects is observed in the application of the static load. In other words, relaxation processes take place prior to failure. These effects are especially severe when the static load is applied in mode *I*. The presence of delayed failure in mode *I* at high loads is an indication of this behavior. It is, therefore, assumed that some relaxation takes place at the crack tip, rendering the actual static loads somewhat less than shown. This is

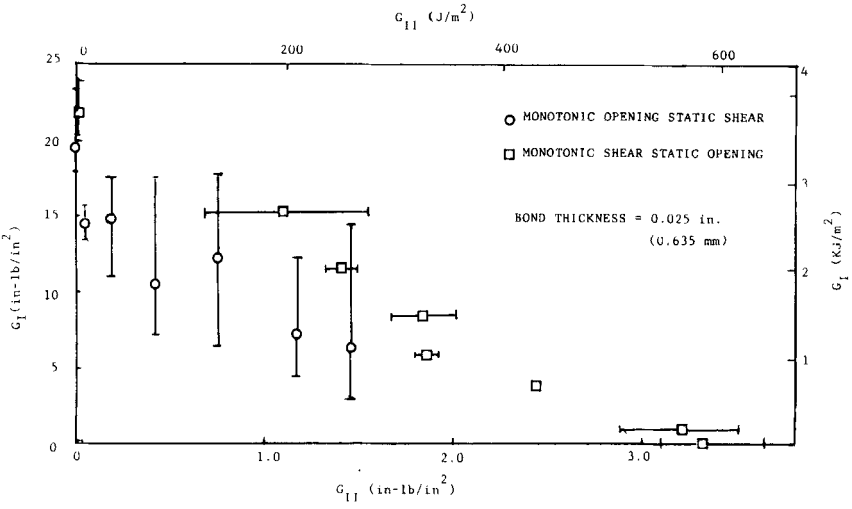

FIGURE 17 G_I *vs.* G_{II} behavior of 0.5 in (12.7 mm) thick specimens bonded with 1113-2 adhesive.

why the data obtained using geometry *B* lie above those obtained using geometry *A* when the P_{II} values are the same in magnitude (note that their mode of application is different). The use of data from both geometries *A* and *B* in determining the failure criteria is thought to have some averaging effect on this behavior.

2) The parabolic (principal stress) criterion defined by Eq. (16) consistently provides a better fit to the experimental data in comparison to the elliptical criterion given by Eq. (14).

The G_I *vs.* G_{II} behavior for the Metlbond 1113-2 adhesive is shown in Figure 17.

CONCLUSIONS

The application of the elastoplastic fracture behavior assumption proved adequate and useful for the model adhesives under study. Excellent correlation was obtained between the properties measured using bulk and bonded specimens. The concept of a plastic deformation zone proves especially useful in determining the optimum adhesive thickness in bonded samples.

The results presented in this paper reveal that when the energy balance criterion is used, the mixed *I–II* mode fracture energy (total energy) values of failure for combined cleavage and shear loading are lower than mode *I* (pure cleavage) fracture energy values at failure. Consequently, G_{IC} is not a sufficient criterion for the failure analysis of adhesively bonded joints. This finding corroborates similar conclusions reported earlier by Bascom *et al.*[18]

Another important conclusion that can be drawn from the data presented is the necessity for considering a maximum principal stress criterion for "brittle" adhesives such as Metlbond. Obviously, the data could be correlated better with the use of a principal stress criterion in comparison to an energy balance criterion. The applicability of a principal stress criterion to ductile adhesives or to glassy polymers subjected to high temperatures, however, is still not known.

The experimental data reveal that the fracture resistance of the model adhesive without the carrier cloth is higher than the fracture resistance of the same adhesive with the carrier cloth in both bonded (mixed mode) and bulk (cleavage only) modes.

The successful application of ILMMS geometry in testing large number of samples should be considered the most important contribution of this work. The physical separation of opening and in-plane shear loads while they are being applied simultaneously allows determination of a failure criterion on the basis of applied loads. Consequently, it becomes possible to compare the failure behavior of different adhesives under similar conditions or to assess the failure behavior of an adhesive under different environmental conditions without calculating any strain energy release rate or stress intensity values.

Acknowledgments

The material covered in this paper is based upon work supported by the National Science Foundation under grants No. CME-8007251 and CEE-8317428. Mr. J. Baldwin's first place award for his work based on this project, earned in the American Institute of Aeronautics 1986 National Graduate Student Competition, is also acknowledged.

References

1. D. W. Dwight, E. Sancaktar and H. F. Brinson, in *Adhesion and Adsorption of Polymers* (Plenum Press, New York, 1980), pp. 141–164.
2. H. F. Brinson, M. P. Renieri and C. T. Herakovich, *ASTM STP* 593, 177 (1975).
3. W. D. Bascom, R. L. Cottington and C. D. Timmons, *J. Appl. Polym. Sci.* **32,** 165 (1977).
4. L. J. Hart-Smith, *Design and Analysis of Adhesive Bonded Joints,* McDonnell-Douglas Co. Report No. 6059A (1972).
5. E. J. Ripling, S. Mostovoy and R. L. Patrick, *ASTM STP* **360,** 5 (1963).
6. *Annual Book of ASTM Standards* (ASTM, Philadelphia, 1984), Vol. 03.01, Designation: E 399–83, pp. 519–554.
7. E. Sancaktar, H. Jozavi and R. M. Klein, *J. Adhesion* **15,** 241 (1983).
8. G. R. Irwin, *Proc. 7th Sagamore Conf.,* pp. IV, 63–173 (1960).
9. D. Broek, *Elementary Engineering Fracture Mechanics,* 3rd. ed. (Noordhoff International Publishing, Leyden, Netherlands, 1974), Chap. 5, p. 116.
10. S. Mall, W. S. Johnson and R. A. Everett, *Cyclic Debonding of Adhesively Bonded Composites,* NASA Tech. Memo. 84577, Nov. 1982.
11. A. J. Kinloch, *Developments in Adhesives-2* (Applied Science Publishers, London, 1981), Chap. 3, pp. 83–124.
12. A. J. Kinloch and S. J. Shaw, *J. Adhesion* **12,** 59 (1981).
13. F. Sezepe, *Proc. 2nd SESA Int. Congress on Exp. Mech.,* pp. 478–484 (1965).
14. B. Gross, J. E. Srawley and W. F. Brown Jr., *Stress Intensity Factors for a Single-Edge-Notched Tension Specimen by Boundary Collocation of a Stress Function,* NASA Tech. Note D-2395, Aug. 1964.

15. W. S. Johnson and P. D. Mangalgiri, *Influence of the Resin on Interlaminar Mixed-Mode Fracture,* NASA Tech. Memo. 87571, July 1985.
16. H. Jozavi and E. Sancaktar, *J. Adhesion* **18,** 25 (1985).
17. D. G. O'Conner, *Factors Affecting the Fracture Energy for a Structural Adhesive,* M.S. Thesis, V.P.I. and S.U. Blacksburg, Virginia, Aug. 1979.
18. W. D. Bascom, R. L. Jones and C. O. Timmons, in *Adhesion Sci. and Tech., Vol. 9B* (Plenum Press, New York, 1975), pp. 501–511.